JOURNAL OF SPACECRAFT AND ROCKETS
Vol. 37, No. 3, May–June 2000

Modeling of a Pulsed Plasma Thruster from Plasma Generation to Plume Far Field

Iain D. Boyd* and Michael Keidar†
University of Michigan, Ann Arbor, Michigan 48103
and
William McKeon‡
Cornell University, Ithaca, New York 14853

Models are presented for a Teflon®-fed, pulsed plasma thruster from plasma generation to plume far field. A one-dimensional model using local thermodynamic equilibrium is developed to describe the plasma generation, Teflon ablation, and nozzle acceleration processes. A computer code that uses two different particle methods is employed to simulate the unsteady plasma plume expansion processes, including charge exchange collisions. Results are generated for a pulsed plasma thruster under development at the University of Illinois. General features of the plume reveal substantial differences in the expansion dynamics of the charged and neutral species. In addition, there is a noticeable difference between the behavior of the carbon and the fluorine ions. Direct comparisons are made between simulation results and experimentally measured data for electron number density and plasma potential. These comparisons indicate strengths and weaknesses of the models.

Introduction

PULSED plasma thrusters are receiving renewed attention because of their ability to produce small impulse bits with high reliability.[1] An accurate simulation of plumes from all electric propulsion devices is required for the assessment of spacecraft integration effects. For a pulsed plasma thruster (PPT) using solid Teflon® as a propellant, the primary integration concern is the deposition of highly condensible plume effluent on spacecraft surfaces.

The numerical investigation of PPT plumes presents many difficulties. The ablation process that leads to the acceleration of a high-density plasma is not well understood. The chemical composition of the flow exhausting from the thruster is not known. The plasma density is significantly higher than that produced by gridded ion thrusters and Hall thrusters. The neutral density at the exit places the flow in the near-continuum regime. Finally, as a result of the pulsed nature of the device, all flow processes are unsteady.

In this study, the focus is on a pulsed plasma thruster called PPT-4 that is under development at the University of Illinois.[2] The PPT-4 is unusual in that the thrust force is generated primarily by an electrothermal mechanism. In terms of modeling, this is a convenient place to start because difficulties with the modeling of the electromagnetic effects can be omitted.

Details of the PPT-4 thruster are first described. This paper reports on two modeling efforts for this device. The first is concerned with modeling the plasma generation, Teflon decomposition, and nozzle acceleration processes. A one-dimensional model is described. The main goal of this study is to provide time-varying boundary conditions for the subsequent computation of the PPT plume. The plume modeling based on particle methods is then described. Results concerning the general flow features of the plume are presented. In addition, direct comparisons are made between simulation and experiment for electron number density and plasma potential. These comparisons serve to partially validate the modeling and also indicate areas where further development is needed.

Presented as Paper 99-2300 at the AIAA/ASME/SAE/ASEE 35th Joint Propulsion Conference, Los Angeles, CA, 20–24 June 1999; received 10 August 1999; revision received 29 November 1999; accepted for publication 8 December 1999.

*Associate Professor, Department of Aerospace Engineering. Senior Member AIAA.
†Research Associate, Department of Aerospace Engineering. Member AIAA.
‡Graduate Research Assistant, Department of Mechanical and Aerospace Engineering. Student Member AIAA.

University of Illinois PPT-4

The thruster under consideration is being developed at the University of Illinois and is called the PPT-4. A schematic diagram is shown in Fig. 1. The PPT-4 has a coaxial configuration with a central anode that is 5 mm in diameter and an annular cathode that is 43 mm in diameter. The two electrodes are connected with a 30-deg half-angle nozzle. The Teflon is ablated from a cylindrical cavity with a diameter of 5 mm and a length of 3.2 mm that sits just in front of the central electrode. The measured mass ablation is 12 μg per pulse at 9 J of input energy. The pulse length is approximately 10 μs. The overall specific impulse has been measured as 1000 s. More details can be found in Ref. 2.

Modeling of Plasma Generation

Pulsed Discharge Model

In the PPT-4, plasma is generated in the Teflon cavity as a result of ionization of the Teflon ablation products. The main features of the discharge in the Teflon cavity are analogous to ablation controlled arcs.[3–5] During the pulse impulse, the plasma is heated by the joule heat and is cooled by radiation, energy losses caused by particle convection to the anode and dielectric, and ionization. This interaction of the plasma column with the walls of the cavity heats the walls rapidly. The temperature of the surface layer increases and reaches the critical temperature of decomposition. The principal mechanism of thermal degradation of the dielectric is the breaking of the bonds in the chain, which consumes the main portion of the energy transferred. As a result of heating, dissociation, and ionization of the products of decomposition, the electron density in the cavity increases. The pressure and temperature of the plasma in the cavity determine the plasma composition. In this section we briefly describe the model of the pulsed electrical discharge in the Teflon cavity. A more detailed description of the model can be found in Ref. 6.

A simplified model of the pulsed discharge in the dielectric cavity is based on the following assumptions: 1) all plasma parameters are uniform within the plasma column; that is, a diffuse type of discharge is assumed; 2) the plasma is quasineutral; and 3) the plasma column is in local thermodynamic equilibrium (LTE), and the electrons, ions, and neutrals establish a single equilibrium temperature. As a result of the foregoing considerations and assumptions, the

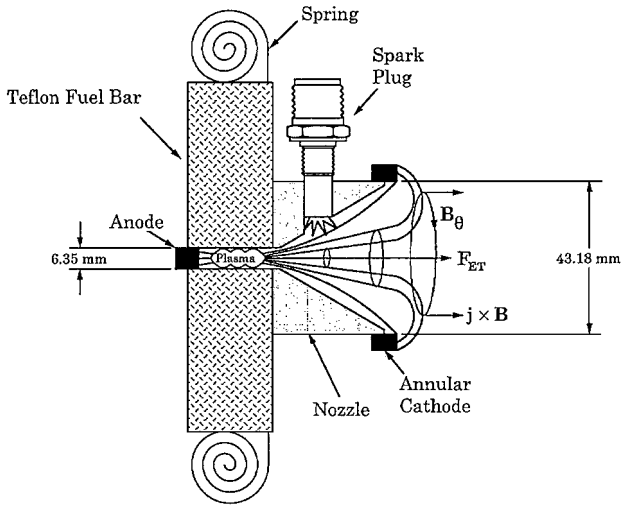

Fig. 1 Schematic diagram of the Illinois PPT-4.

following energy balance equation in the quasi-neutral plasma column can be written:

$$\frac{3}{2}n_e\frac{\mathrm{d}T}{\mathrm{d}t} = Q_j - Q_r - Q_d - Q_a \tag{1}$$

where n_e is the electron density, T is the plasma temperature, Q_j is the joule heat, Q_r is the radiative emission energy loss that depends on plasma density and temperature, Q_d is the energy loss caused by convection of electrons and ions to the dielectric that depends on the plasma temperature and the potential drop in the electrostatic sheath near the dielectric, and Q_a is the energy loss caused by electron convection to the anode that depends on the anode sheath potential drop.

The anode current is carried by electrons and controlled by the potential drop in the anode sheath. The potential drop in the sheath depends on the plasma and current density and may have spatial variation. Assuming that the plasma column is uniform, generally, the sheath is slightly negative in order to repel the excess of the thermal electron current, so that the electron current to the anode is equal to the circuit current. Similar physical reasons lead to the appearance of the electrostatic sheath near the dielectric surface to ensure a zero net current. The transient sheath formation near the dielectric surface is determined by the dielectric permittivity. In the considered range of electron density (10^{21}–10^{24} m^{-3}), the characteristic charging time[7] is less than 10^{-10} s, which is much smaller than the characteristic time of the discharge parameter changes. Therefore we use a quasi-steady-state sheath model. Furthermore, we assume that the plasma density is so high that the sheath thickness (of the order of the Debye length) is much smaller than the electron Larmor radius and thus the effect of the self-magnetic field in the sheath can be neglected. As in the case of the anode sheath, the sheath potential drop should be negative in order to repel the excess of the thermal electron current, so that the electron current is equal to the ion current.

In LTE, the composition of the plasma is found as a function of the state of the plasma that is determined by the pressure and temperature. The calculation of the composition of the plasma consists of solving a set of Saha equations supplemented by a pressure balance, conservation of nuclei, and quasineutrality. It is assumed that the plasma pressure is equal to the equilibrium vapor pressure based on the temperature of the Teflon surface.[8] The Teflon surface temperature is calculated by the solution of the heat transfer equation. This equation is subject to the boundary conditions at the Teflon surface accounting for heat flux from the plasma by radiation and particle convection and heat losses caused by evaporation of the surface. In the cavity, the plasma velocity changes from zero near the anode up to a value equal to the local velocity of sound at the cavity outlet. The considered plasma flow problem inside the cavity is, in principle, two dimensional. However, in the main part of the plasma bulk, the two-dimensional effect is small.[9] In the cavity, the plasma velocity varies from zero near the anode up to the sound speed at the cavity exit plane, and thus the plasma density should decrease toward the cavity exit plane. However, if ablation is approximately uniform along the cavity, the plasma velocity increases substantially only near the exit (at approximately 80% of the cavity length, as shown in Ref. 9). A quasi-steady analysis[9] shows that, in the plasma bulk, the velocity is approximately $(0.3–0.5)C_s$, where C_s is the sound speed. Therefore the plasma velocity was used in the model as a free parameter. It was found that the plasma velocity does not significantly affect the plasma density and temperature distributions during the discharge pulse.

Plasma Acceleration in the Conical Nozzle

The electromagnetic thrust component of the PPT-4 is created mainly near the thruster exit plane, where the azimuthal self-magnetic field and the radial component of the discharge current are maximal. However, the current pulse is essentially gone before the main plasma cloud exits from the cavity. Thus, the main part of the plasma generated in the cavity accelerates in the conical nozzle by the gasdynamic mechanism. In this section we describe a quasi-one-dimensional model of a continuum, single-fluid plasma flow in the conical nozzle neglecting magnetic field effects.

We consider a quasi-neutral plasma in which the electrons and ions behave as ideal gases. The plasma temperature is assumed to be constant. This is based on the idea that the effects on the temperature of gasdynamic expansion and plasma ohmic heating will almost cancel. The temperatures obtained by using our approach (between 1 and 3 eV) are in good general agreement with values measured experimentally in the plume.[2] The plasma flow is considered to be sourceless, and plasma losses to the nozzle wall and wall evaporation are neglected. Furthermore, we consider the situation in which all properties vary only along the axial direction. The plasma jet cross section $A(z)$ is determined by the nozzle geometry as follows:

$$A(z) = A_0[1 + (z/R_0)\tan\theta]^2 \tag{2}$$

where A_0 is the initial cross section, R_0 is initial jet radius equal to the cavity radius, and θ is the cone half-angle. Taking into account these considerations, we find the equation for the plasma velocity becomes

$$\frac{V^2 - C_s^2}{V}\frac{\mathrm{d}V}{\mathrm{d}z} = C_s^2\frac{2\tan\theta}{R_0}\frac{1}{1 + (z/R_0)\tan\theta} \tag{3}$$

where V is the plasma jet axial velocity.

Time-Dependent Nozzle Exit Conditions

Here we present results of the calculation of the plasma parameters at the exit plane of the PPT-4. To simulate the energy input during the pulse, the experimental current waveform has been used.[2] Linearization of the experimental current waveform causes some perturbations in the results presented later. The calculations presented in this section correspond to the following PPT-4 design and discharge parameters: cavity size $R_a = 3.15$ mm, $L = 8.3$ mm, nozzle half-angle $\theta = 30$ deg, current peak ~ 8 kA, and pulse duration ~ 10 μs.

During the discharge pulse, plasma is generated in the cavity as a result of Teflon decomposition and then accelerates in the conical nozzle. The solution of the energy and mass balance equations provides time dependencies of the plasma temperature and composition in the cavity. During the plasma flow in the nozzle, plasma composition and temperature remain constant while plasma velocity increases starting from the sound speed at the cavity exit plane. In the conical nozzle, plasma acceleration up to a Mach number of 4 is calculated.

The time evolution of the plasma component densities, temperature, and velocity are shown in Figs. 2a–2c. The chemical composition of the plasma is shown in Fig. 2a. One can see that all densities peak at ~ 6 μs, which corresponds to the peak of the discharge current. The fluorine (F) neutral density is larger than the carbon (C) neutral density because Teflon has a composition of C_2F_4. However, the difference between fluorine ion density and carbon ion density is much smaller because carbon has a smaller ionization energy.

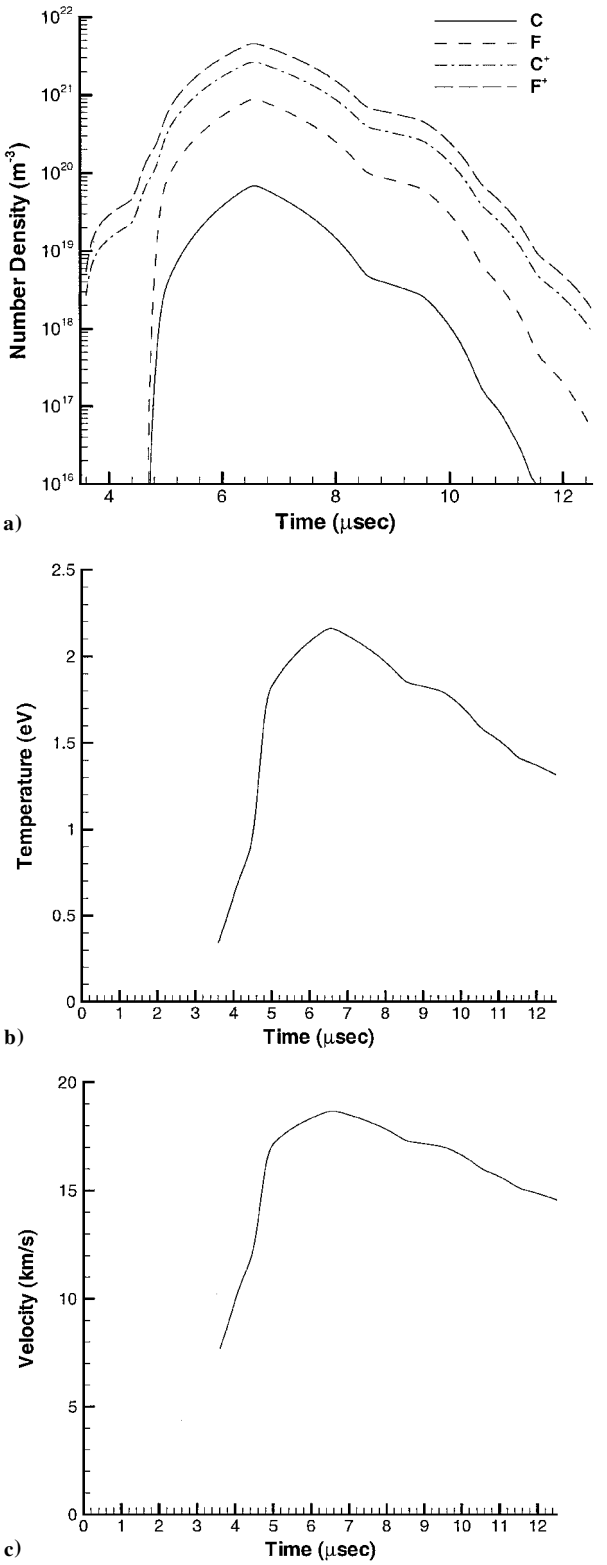

Fig. 2 Variations with time of a) species number densities, b) electron temperature, and c) velocity at the thruster exit plane.

(The first ionization energy of carbon is 11.3 eV, whereas fluorine has a corresponding ionization energy of 17.4 eV.) Initially, the plasma temperature sharply increases and peaks at ~2.3 eV. Toward the pulse end the plasma temperature decreases down to ~1.5 eV. These profiles are used as time-varying boundary conditions for the plasma plume simulations.

Plume Model

A computer model for PPT plumes has been proposed by Yin and Gatsonis.[10] A hybrid fluid–particle approach was employed. In the present study, we employ a similar approach. Neutrals (C and F) and ions (C^+ and F^+) are modeled as particles. Particle collisions are computed by using the direct simulation Monte Carlo method (DSMC).[11] Both momentum exchange and charge exchange collisions are simulated. Momentum exchange cross sections use the model of Dalgarno et al.,[12] and the collision dynamics follows the normal DSMC procedures as described in Ref. 11. The charge exchange processes use the cross sections proposed by Sakabe and Izawa.[13] The computer code uses separate grids for the collision and plasma processes. The cells used for the collisions are sized according to the local mean free path, as is the usual case in DSMC computations. The experimental facility backpressure corresponds to a density of $\sim 10^{18}$ m^{-3}. This is applied as an auxiliary condition with which particles from the thruster can collide.

Acceleration of the charged particles in self-consistent electric fields is simulated by using the particle-in-cell method (PIC).[14] The plasma potential ϕ is obtained by assuming charge neutrality to determine the electron number density from the total ion density. The electron number density n_e is then used in the Boltzmann relation to obtain the plasma potential:

$$\phi = T_e \ln[n_e / n_{\text{ref}}(t)] \tag{4}$$

where the electron temperature T_e is in electron volts and n_{ref} is the electron number density at a reference point. This approach was used in our previous work on Hall thruster plumes.[15] In the case of the PPT, the reference point for the Boltzmann relation is taken as the thruster exit. It is assumed that the potential here is constant. The variation of electron number density at the thruster exit obtained in the plasma generation modeling is used to change the reference density as a function of time. A constant electron temperature of 2 eV is used in the Boltzmann relation throughout the computation. Because charge neutrality is assumed, the PIC cells do not have to be of the order of the Debye length. Instead they are chosen to be small enough to resolve in a reasonable way the gradients in the potential. The grids used in the computation are shown in Fig. 3. A single time step given by the reciprocal of the maximum plasma frequency is used throughout. All results are time dependent and are integrated over small intervals of time, which are of the order of 2×10^{-7} s.

The main difficulties in performing the computations of the PPT plume arise from the transient nature of the expansion. Because the flow conditions change as a function of time, the characteristic time and length scales of both collision and plasma phenomena continually change throughout the computational domain. In principle, the simulations should use grids that change with the local, transient flow conditions. In this first study, we have adopted the simpler approach of employing grids that should capture most of the physics most of the time. Another numerical problem related to the transient flow conditions is the fact that there are often regions of the flow where the number of simulated particles is very small. This occurs at the leading edge of the forward expansion at early times and at the trailing edge of the expansion at late times. The low number of

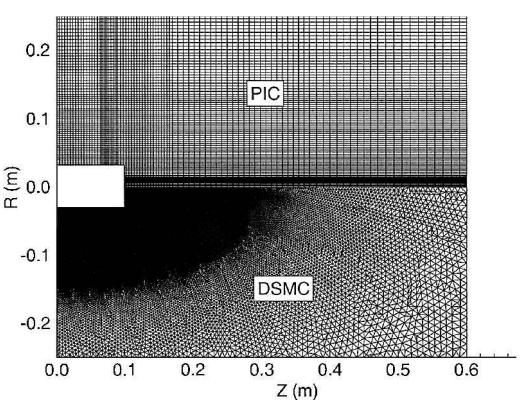

Fig. 3 Computer grids employed in the plume particle simulation.

particles in these regions leads to significant scatter in the simulation results in these regions. In the early stages of this investigation we experimented with the use of very large computations involving many millions of particles performed on parallel computers. This approach only moved the statistical scatter to lower density portions of the flowfield. As shown in the Results section, the density varies by several orders of magnitude across the jet expansions and so the statistical problem is unavoidable. It should be noted, however, that most of the results presented are unaffected by the statistical fluctuations.

Results

Particles are introduced into the flowfield through the nozzle exit plane by using the output from the plasma generation model (Fig. 2). A uniform radial profile of properties is assumed across the exit plane except that a conical distribution of flow angle is used. Ions and neutrals are assumed to have the same velocity and the same temperature. This assumption is based on the fact that the number densities are relatively high so that the frequency of charge exchange collisions inside the nozzle is high. Simulations are performed with and without the facility backpressure. It is found that the results are almost identical, indicating that, unlike some other electric propulsion devices such as Hall thrusters and ion thrusters, the PPT plume is not affected by the chamber background gas.

To illustrate some of the basic dynamics of the time evolution of the PPT plume expansion processes, Figs. 4a–4d show contours of plasma potential at four different times. In these results it is clear that the plasma potential expands very rapidly about a source that moves with the plume. The gradients in potential are such as to create electric fields that will accelerate ions: 1) in the forward direction at the front of the expansion; 2) in the backward direction at the rear end of the expansion, which results in backflow of ions behind the thruster; and 3) in the radial direction away from the axis. Of course, these forces act only on the charged particles; thus in the results that follow, it is expected that the ions will behave quite differently from the neutral atoms.

To demonstrate the different dynamics of ions and neutrals, Figs. 5a–5d show the variation of all species densities along the axis at four different times. As shown in Fig. 5a, at 10 μs after ignition, the species densities follow the profiles shown in Fig. 2a. The ions are in a larger concentration than the neutral atoms, and fluorine is more abundant than carbon. The relative concentrations of the species do not change dramatically at later times as shown in Figs. 5b–5d. However, the shape of the profiles reveals that the charged species are spread over a larger axial region than the neutrals. The neutral atoms expand as a relatively compact puff of gas, whereas the ions are spread out both ahead of and behind the center of expansion as a result of electric field effects.

Comparisons between the computation and experimental measurement[2] of the electron number density along the axis are shown at three different locations in Figs. 6a–6c. Because charge neutrality is assumed, the computational results are obtained by summing the carbon and fluorine ion densities. When a comparison is made with the experimental data, it is expected that the data collected over the first 10 μs after ignition cannot be used. This is partly because of the noise introduced into the measurements by the operation of the spark plug igniter. In addition, there is no attempt in our modeling to simulate the behavior of the ignition plasma. With

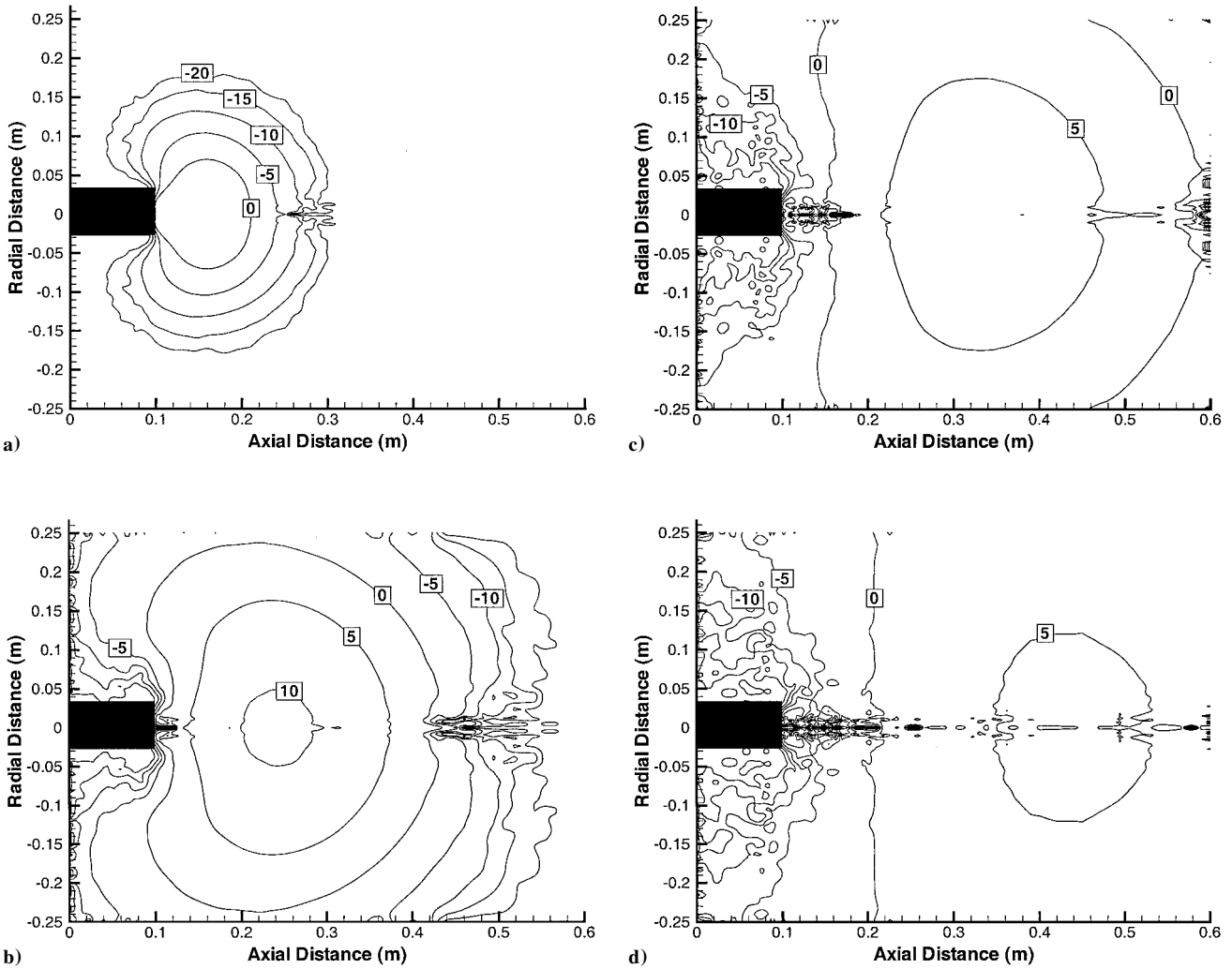

Fig. 4 Contours of plasma potential in volts: a) 10, b) 15, c) 20, and d) 25 θ s after ignition.

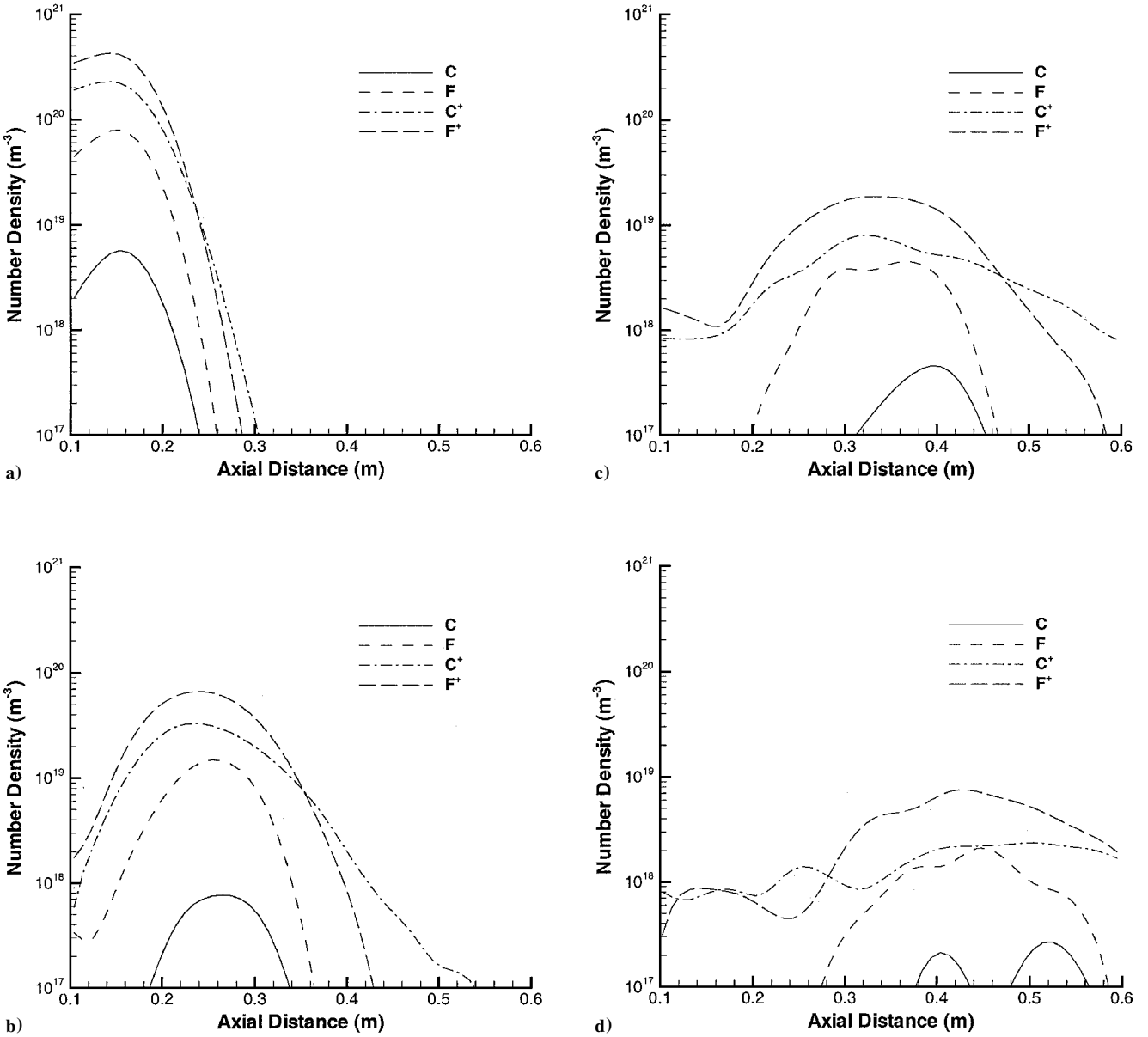

Fig. 5 Profiles of species number density along the axis: a) 10, b) 15, c) 20, and d) 25 θ s after ignition.

this in mind, we can make two clear observations about the comparisons shown in Fig. 6. The first is that there is a tendency in the simulations to overpredict the density peak. However, it should be noted that the experimental uncertainty is ±50% and the predicted peaks lie within this range. There also appears to be some indication of saturation in the experimental measurements. It is surprising to see such a small reduction in the peak density measured at 10 and 14 cm from the thruster. The second clear conclusion is that the simulation underpredicts the densities at both early and late times.

A comparison of the simulation results with experimental data shows that the main plasma plume features are captured, although the simulation underestimates the densities at long times. The underprediction of the plasma density at long times is a result of the basic assumption of the plasma generation model in considering the plasma to be uniform in the cavity. This approach means that the plasma properties are described by average plasma parameters. Thus, this model predicts that the plasma will leave the cavity after the pulse end in a time that is short compared with the pulse duration. In general, however, the problem is two dimensional, with plasma velocity and density variation in the radial and axial directions. The plasma velocity varies from zero near the central electrode up to the sound speed at the cavity exit plane. After the pulse ends, there is a substantial reduction in the ablation rate and the plasma density in the cavity will decrease. Plasma density temporal decay in this case will be much slower than that in the present model. In the future, this effect will be included in our model by considering spatial variation in the cavity properties.

To predict the chemical composition of the plasma, the present model uses the Saha equation assuming local thermodynamic equilibrium in the plasma column. However, LTE may be established only in relatively dense plasmas with an electron number density greater than 10^{22} m^{-3} for a time period larger than the characteristic relaxation time for ionization and recombination in the plasma (of the order of 10^{-7} s; Ref. 16). Calculations show that during the main part of the pulse, these requirements are fulfilled. Toward the pulse end, however, the plasma density significantly decreases and the relaxation time becomes comparable with the pulse duration. Thus, toward the pulse end, the LTE approach predicts a plasma ionization degree that is much higher than it should be in the real situation.

In Figs. 7a–7c a comparison is made between measurements and computations for the plasma potential on the axis at the same three

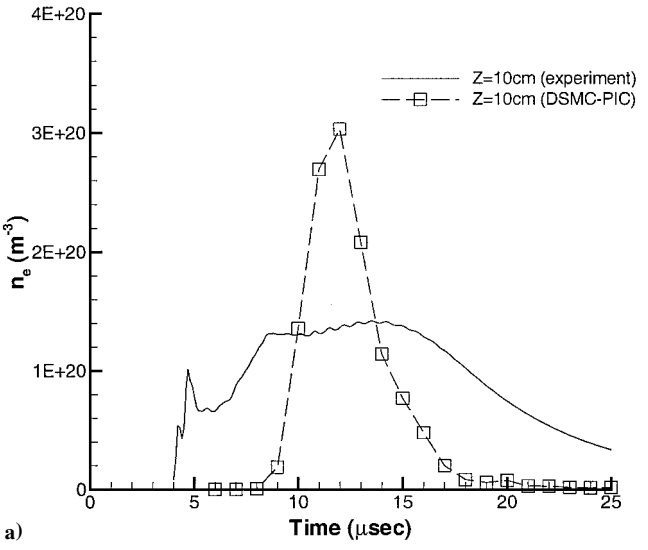

a)

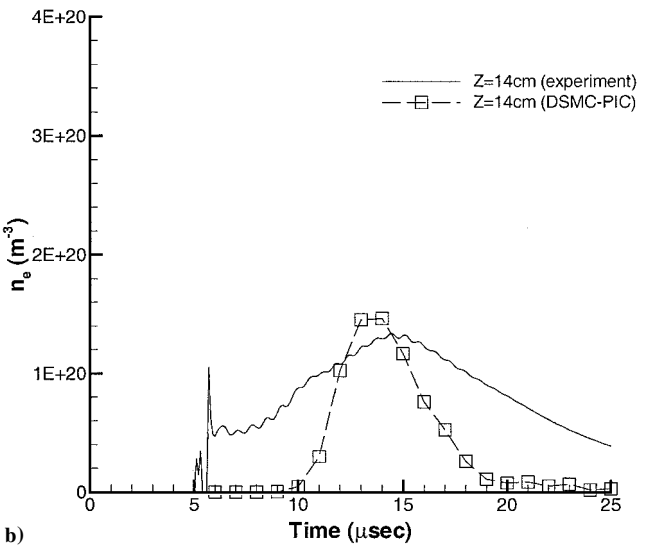

b)

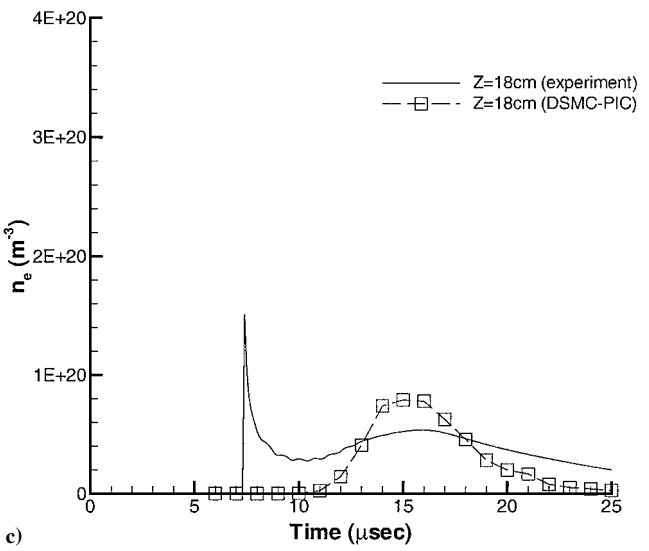

c)

Fig. 6 Profiles of electron number density on the axis: a) 10, b) 14, and c) 18 cm from the thruster.

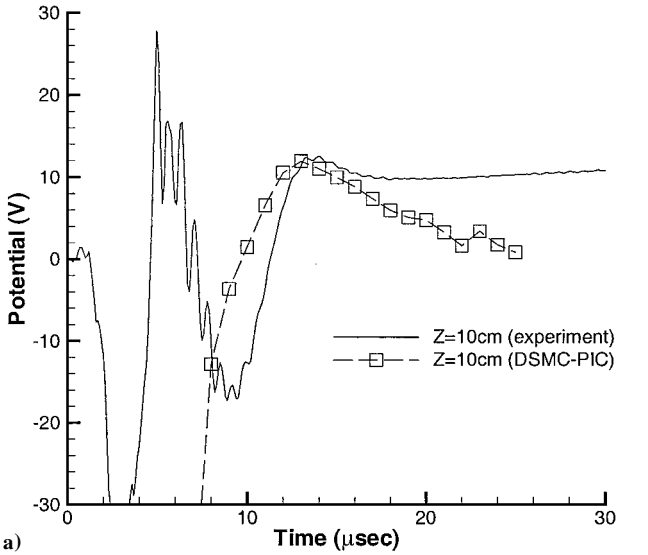

a)

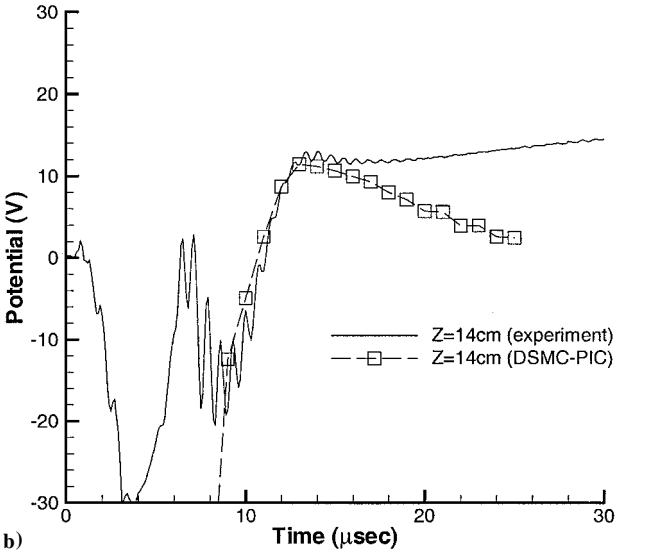

b)

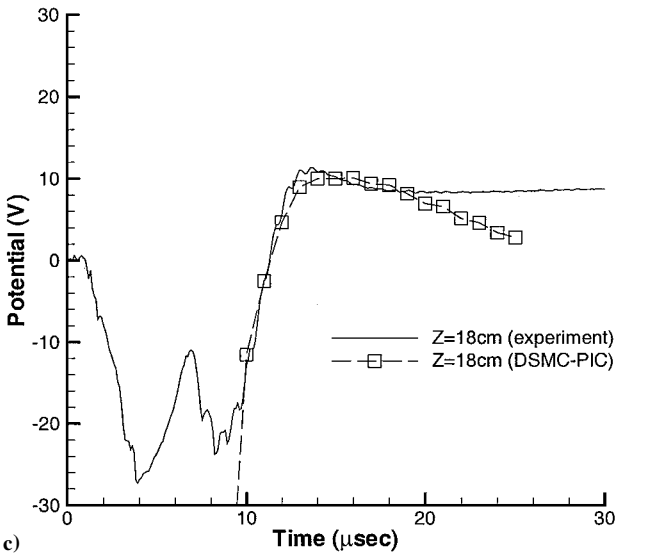

c)

Fig. 7 Profiles of plasma potential on the axis: a) 10, b) 14, and c) 18 cm from the thruster.

locations as considered in Fig. 6. If we again ignore the first 10 μs, we can see that the initial rise and the actual peak of the potential data at all three locations is well predicted by the simulation. Also, consistent with the electron number density comparisons, the simulations show a more rapid decay in potential at long times after ignition. Overall, the comparisons with the experimental data shown in Figs. 6 and 7 indicate that the modeling has achieved a reasonable level of success.

As mentioned earlier, the primary reason for performing plume computations of the PPT is to assess possible spacecraft interaction effects. With this in mind, we present in Figs. 8 and 9 mass flux results as a function of time from the simulations in the radial planes at 50 cm forward of the thruster exit and above the thruster exit, respectively. The latter plane is chosen to assess the potential backflow problem. The forward contamination problem could occur if PPTs are employed on closely spaced spacecraft flying in formation. Figure 8 indicates that the mass flux at any plane changes dramatically as a function of time. As shown in Fig. 8a, the earliest flux consists of the fastest ions that are accelerated electrostatically ahead of the neutrals. Because the charge-to-mass ratio of carbon is about 50% larger than that for fluorine, it is the carbon ions that are the first species to impact a surface forward of the thruster. Figure 8b indicates that any significant flux of neutral atoms is delayed by $\sim$5 μs in reaching the surface and even then the flux magnitude is $\sim$2 orders of magnitude below that of the ions. At later times, the radial acceleration of ions leads to their relative magnitudes of mass flux becoming comparable with that of fluorine atoms. The mass flux of carbon atoms remains at a lower level up until 35 μs.

The backflow contamination issue is demonstrated in Fig. 9, and this phenomenon would be of concern on any spacecraft using PPTs. Relative to ion thrusters and Hall thrusters, the potential for backflow with PPTs is significantly higher. This occurs because the carbon and fluorine ions are significantly more mobile than xenon and because the neutral and ion densities are orders of magnitude higher for the PPT, leading to increased collisional scattering. In the simulations, almost no backflow of neutral atoms is predicted. The peak mass flux occurs soon after ignition as shown in Fig. 9a, and the maximum level is only 1 order of magnitude below the maximum found in Fig. 8 for the forward fluxes. Again because of their increased mobility, carbon ions dominate the backflow flux. At later times, it can be seen that the mass flux decreases dramatically.

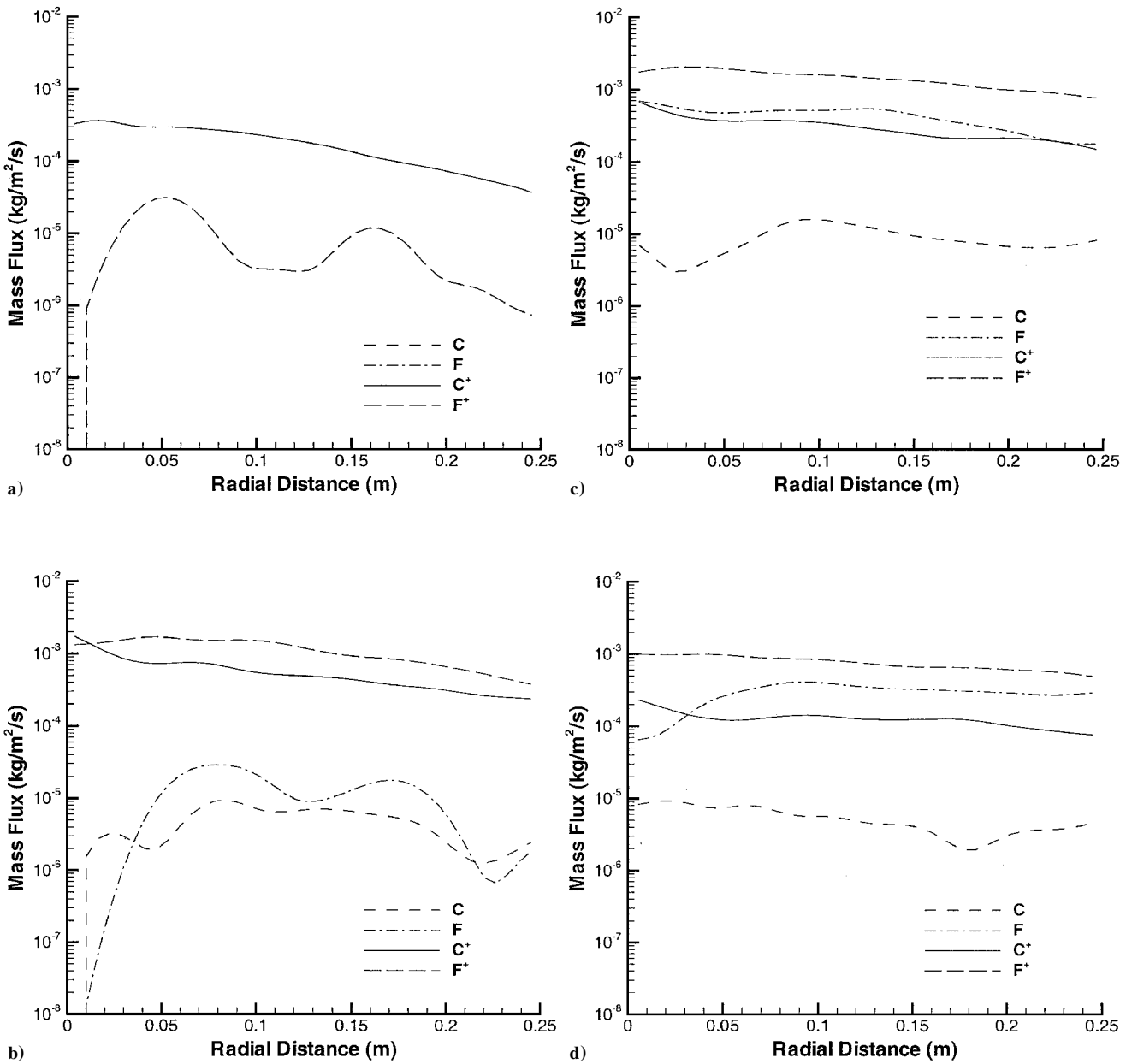

Fig. 8 Forward flow mass flux in the plane at 50 cm from the thruster exit: a) 20, b) 25, c) 30, and d) 35 θ s after ignition.

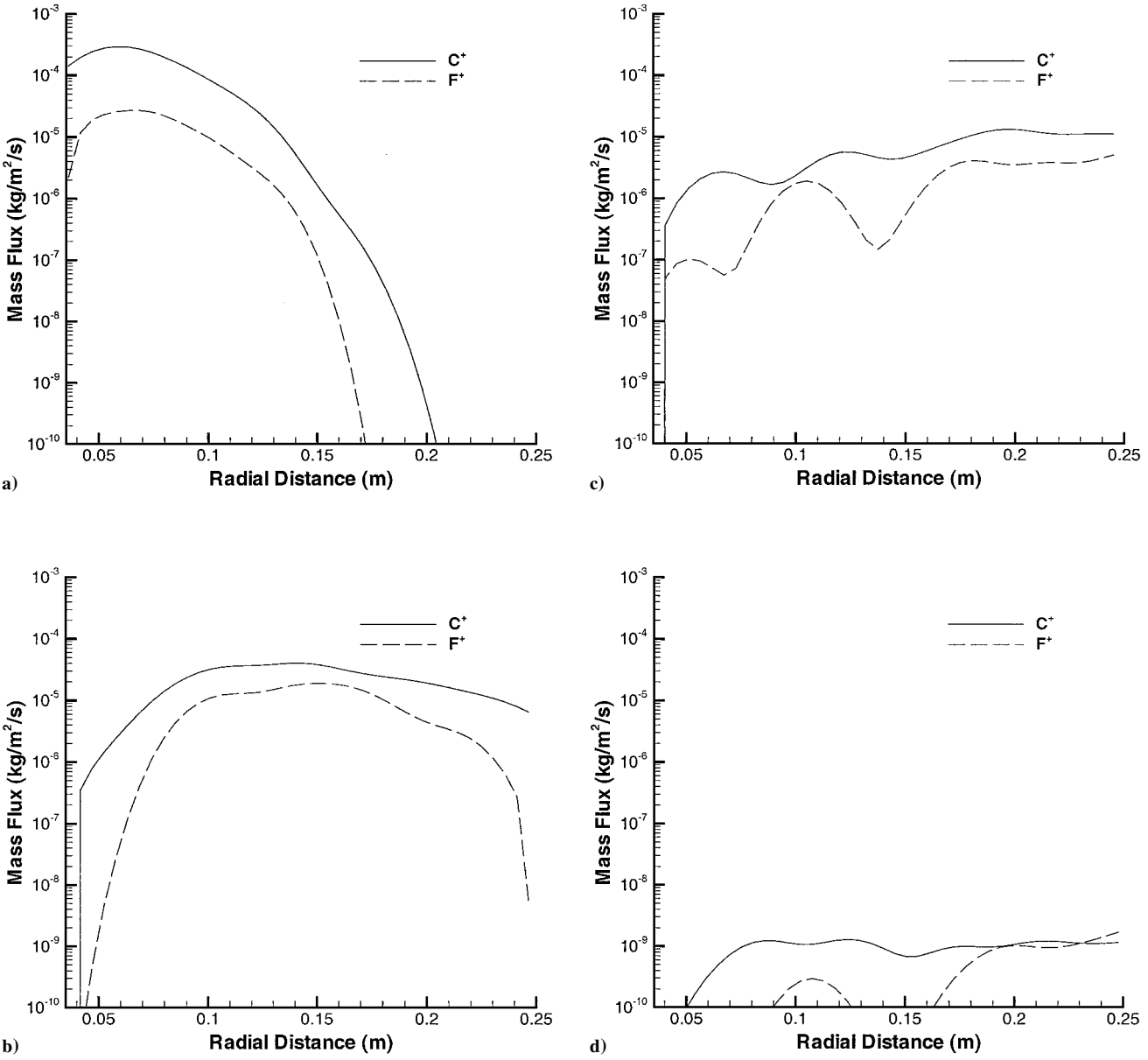

Fig. 9 Backflow mass flux in the plane above the thruster exit: a) 10, b) 15, c) 20, and d) 25 θ s after ignition.

Conclusions

A model has been developed to describe the plasma processes of a Teflon-fed pulsed plasma thruster from plasma generation to plume far field. The device considered was the PPT-4, which is being developed at the University of Illinois. From the modeling standpoint, this is an interesting thruster, as the acceleration is generated primarily by electrothermal effects.

The plasma generation, Teflon ablation, and nozzle expansion were modeled by using a one-dimensional approach. Local thermodynamic equilibrium was used to compute the chemical composition. A quasi-steady assumption was made to compute the nozzle flow. The time-dependent properties computed at the nozzle exit were used as boundary conditions for a separate plume computation.

The plume computation used a combination of the PIC and DSMC method to compute the plasma and collision phenomena in the expanding plume. The computations of plasma potential indicated that the ions are accelerated ahead of the expanding plume, radially away from the axis, and backward behind the thruster. It was found that, as a result of electric field effects, the dynamics of the ions and that of the atoms in the plume were substantially different. In addition, because of a relatively large difference in the charge-to-mass ratio, the dynamics of the carbon and that of the fluorine ions were also perceptibly different. It was found that the primary source of backflow contamination from the thruster was carbon ions. The forward contamination was found to be time dependent, with an initial flux of ions followed by a later flux of neutral atoms.

Comparisons were made between the computations and experimental measurements taken at the University of Illinois for the plasma potential and electron number density. In general, the agreement between the data sets was very good. It was found that, at late times, the computations predicted a more rapid decay in both potential and electron number density in comparison with the measured data. This suggested improvements in the plasma generation model that will be investigated further. The good agreement obtained between predictions and measurements provides confidence in the overall modeling approach used in this study.

Acknowledgments

Funding for this work was provided by the Air Force Office of Scientific Research under Grant F49620-99-1-0040 with Mitat A. Birkan as Monitor. We thank Rod Burton and Stu Bushman from the University of Illinois for explaining details of the PPT-4 to us and for sharing their experimental data.

References

[1]Burton, R. L., and Turchi, P. J., "Pulsed Plasma Thruster," *Journal of Propulsion and Power*, Vol. 14, No. 5, 1998, pp. 716–735.

[2]Bushman, S. S., "Investigations of a Coaxial Pulsed Plasma Thruster," M.S. Thesis, Univ. of Illinois, Urbana, IL, 1999.

[3]Ogurtsova, N. N., Podmoshenskii, I. V., and Rogovtsev, P. N., "Calculation of the Parameters of an Optically Dense Plasma Obtained by a Discharge with an Evaporating Wall," *High Temperature*, Vol. 9, 1971, pp. 430–436.

[4]Kovatia, P., and Lowke, J. J., "Theoretical Prediction of Ablation Stabilised Arcs Confined in Cylindrical Tubes," *Journal of Physics D: Applied Physics*, Vol. 17, 1984, pp. 1197–1212.

[5]Ruchti, C. B., and Niemeyer, L., "Ablation Controlled Arc," *IEEE Transactions in Plasma Science*, Vol. 14, No. 4, 1986, pp. 423–434.

[6]Keidar, M., Boyd, I. D., and Beilis, I. I., "Electrical Discharge in the Teflon Cavity of a Co-Axial Pulsed Plasma Thruster," *IEEE Transactions in Plasma Science* (to be published); also International Electric Propulsion Conf., IEPC Paper 99-214, Oct. 1999.

[7]Whipple, E. C., "Potential of Surface in Space," *Report of Progress in Physics*, Vol. 44, 1981, pp. 1197–1250.

[8]Turchi, P. J., "Directions for Improving PPT Performance," International Electric Propulsion Conf., IEPC Paper 97-038, Sept. 1997.

[9]Keidar, M., Boyd, I. D., and Beilis, I. I., "Particulate Interaction with Plasma in a Teflon Pulsed Plasma Thruster," *Journal of Propulsion and Power* (to be published); also International Electric Propulsion Conf., IEPC Paper 99-213, Oct. 1999.

[10]Yin, X., and Gatsonis, N. A., "Numerical Investigation of Pulsed Plasma Thruster Plumes," International Electric Propulsion Conf., IEPC Paper 97-036, Sept. 1997.

[11]Bird, G. A., *Molecular Gas Dynamics and the Direct Simulation of Gas Flows*, Oxford Univ. Press, New York, 1994.

[12]Dalgarno, A., McDowell, M. R. C., and Williams, A., "The Mobilities of Ions in Unlike Gases," *Proceedings of the Royal Society of London*, Vol. 250, April 1958, pp. 411–425.

[13]Sakabe, S., and Izawa, Y., "Simple Formula for the Cross Sections of Resonant Charge Transfer Between Atoms and Their Ions at Low Impact Velocity," *Physical Review A: General Physics*, Vol. 45, No. 3, 1992, pp. 2086–2089.

[14]Birdsall, C. K., and Langdon, A. B., *Plasma Physics Via Computer Simulation*, Adam Hilger, Bristol, England, U.K., 1991.

[15]VanGilder, D. B., Boyd, I. D., and Keidar, M., "Particle Simulations of a Hall Thruster Plume," *Journal of Spacecraft and Rockets*, Vol. 37, No. 1, 2000, pp. 129–136; also AIAA Paper 98-3797, July 1998.

[16]Griem, H. R., *Plasma Spectroscopy*, McGraw–Hill, New York, 1964.

R. G. Wilmoth
Associate Editor